Cyclin G1 Is a Target of miR-122a, a MicroRNA Frequently Down-regulated in Human Hepatocellular Carcinoma

Laura Gramantieri,[1] Manuela Ferracin,[2] Francesca Fornari,[1] Angelo Veronese,[2,3] Silvia Sabbioni,[2] Chang-Gong Liu,[4] George A. Calin,[4] Catia Giovannini,[1] Eros Ferrazzi,[3] Gian Luca Grazi,[1] Carlo M. Croce,[2,4] Luigi Bolondi,[1] and Massimo Negrini[2,4]

[1]Dipartimento di Medicina Interna e Gastroenterologia e Centro di Ricerca Biomedica Applicata, Università di Bologna, Bologna, Italy; [2]Dipartimento di Medicina Sperimentale e Diagnostica e Centro Interdipartimentale per la Ricerca sul Cancro, Università di Ferrara, Ferrara, Italy; [3]Istituto Oncologico Veneto, Rovigo, Italy; and [4]Comprehensive Cancer Center, Ohio State University, Columbus, Ohio

Abstract

We investigated the role of microRNAs (miRNAs) in the pathogenesis of human hepatocellular carcinoma (HCC). A genome-wide miRNA microarray was used to identify differentially expressed miRNAs in HCCs arisen on cirrhotic livers. Thirty-five miRNAs were identified. Several of these miRNAs were previously found deregulated in other human cancers, such as members of the *let-7* family, *mir-221,* and *mir-145*. In addition, the hepato-specific *miR-122a* was found down-regulated in ~70% of HCCs and in all HCC-derived cell lines. Microarray data for *let-7a, mir-221,* and *mir-122a* were validated by Northern blot and real-time PCR analysis. Understanding the contribution of deregulated miRNAs to cancer requires the identification of gene targets. Here, we show that *miR-122a* can modulate cyclin G1 expression in HCC-derived cell lines and an inverse correlation between *miR-122a* and cyclin G1 expression exists in primary liver carcinomas. These results indicate that cyclin G1 is a target of *miR-122a* and expand our knowledge of the molecular alterations involved in HCC pathogenesis and of the role of miRNAs in human cancer. [Cancer Res 2007;67(13):6092–9]

Introduction

Hepatocellular carcinoma (HCC) accounts for 80% to 90% of liver cancers and it is one of the most prevalent carcinomas throughout the world (1). Cirrhosis represents the strongest predisposing factor, as 80% of HCCs develop in cirrhotic livers (2). By assaying HCCs with DNA microarrays, several signaling pathways potentially involved in HCC development and progression through the modulation of multiple mRNAs have been recognized (3). In addition, specific molecular signatures have been associated with different etiologic factors, biological characteristics, and clinical evolution (4, 5). In particular, deregulated expression of protein involved in cell cycle regulation and in DNA repair has extensively been described as a crucial event in the carcinogenetic process leading to HCC development (6).

In the recent years, a new class of small noncoding RNAs, microRNAs (miRNA), has been discovered in animals and plants (7–9). miRNAs are 19- to 25-nucleotide-long RNAs, able to bind complementary sequences in 3′-untranslated regions (3′-UTR) of several target mRNAs to induce their degradation or translational repression (10). They are phylogenetically conserved, play important roles in developmental timing, and participate in the regulation of processes, such as cell fate determination, proliferation, differentiation, and cell death (11–14). In the most recent database (miRBase 9.0), ~500 validated miRNAs are presently identified in the human genome (15), which could regulate thousands of protein-coding genes (16, 17). Most of the protein-coding genes regulated by miRNAs are presently not defined and bioinformatic approaches may help to recognize them.

The development of microarray platforms for the analysis of miRNA expression revealed that multiple miRNAs are aberrantly expressed in human malignancies, suggesting that they may represent a novel class of oncogenes or tumor suppressor genes (18–22). Here, we report a comprehensive analysis of miRNA expression in HCCs arisen on liver cirrhosis (LC). Our data suggest that the aberrant expression of a restricted panel of miRNAs could participate in the molecular events leading to HCC development. Moreover, among deregulated miRNAs, *miR-122a,* which accounts for 70% of the total liver miRNA population (23), was analyzed as a modulator of cyclin G1 expression.

Materials and Methods

Patients. Tissues were obtained from 60 patients (45 males and 15 females) undergoing liver resection for HCC on LC. Tissue samples were collected at surgery, immediately snap frozen in liquid nitrogen, and stored at −80°C until RNA extraction. The characteristics of HCC/LC patients included in this study are described in Table 1. Exclusion criteria were a previous history of local or systemic treatment for HCC and the presence of noncirrhotic tissue surrounding the HCC nodule/s. miRNA expression was analyzed by microarray on 17 HCCs and 21 LCs (matched in 13 cases) by Northern blot on 40 cases of matched HCC/LC and by quantitative real-time reverse transcription-PCR (RT-PCR) on 38 cases of matched HCC/LC. Characteristics of each sample and study details are summarized in Supplementary Tables S1 and S2.

miRNA microarray. Total RNA was extracted by using Trizol (Invitrogen) according to the manufacturer's instructions. One-color RNA labeling and hybridization on miRNA microarray chips was done as described previously (18). For the analysis of miRNA expression profile, 17 HCCs and 21 LCs (matched in 13 cases) were hybridized on a miRNA microarray consisting of 381 probes for 238 mature and 143 precursor human miRNAs. Hybridization signals were detected by biotin binding of a streptavidin-Alexa Fluor 647 conjugate using a GenePix 4000B scanner (Axon Instruments). Images were quantified by the GenePix Pro 6.0 (Axon Instruments).

Analysis of microarray data. Raw data from one-color miRNA microarrays were normalized and analyzed by GeneSpring GX software version 7.3 (Agilent Technologies). The GeneSpring software generated a

Note: Supplementary data for this article are available at Cancer Research Online (http://cancerres.aacrjournals.org/).

Requests for reprints: Massimo Negrini, Dipartimento di Medicina Sperimentale e Diagnostica, Università di Ferrara, via Luigi Borsari 46, 44100 Ferrara, Italy. Phone: 39-0532-291399/291400; Fax: 39-0532-247618; E-mail: ngm@unife.it.

doi:10.1158/0008-5472.CAN-06-4607

unique value for each miRNA, doing the average of replicate probes present on chip. Samples were normalized using the on-chip median normalization. Then, each tumor was normalized on the cirrhosis of the same patient, when available, or on the average of cirrhosis. Differentially expressed miRNAs were identified by using a filter based on a fold change of 1.3 combined with an ANOVA for HCCs versus cirrhosis comparison ($P < 0.05$) with Benjamini and Hochberg correction for false-positive reduction. The list of differentially expressed genes was tested for its prediction power with the algorithms prediction analysis of microarrays (PAM; ref. 24) and support vector machine (SVM; ref. 25). Unsupervised hierarchical cluster analysis was done after median centering of each chip using average linkage and standard correlation as measure of similarity. Supervised clusterization was done after the normalization on gene median to highlight differences across samples.

Northern blot analysis. RNA samples (10 μg each) were electrophoresed on 15% acrylamide and 7 mol/L urea Criterion precasted gels (Bio-Rad) and transferred onto Hybond N+ membrane (Amersham Biosciences). Membranes were hybridized with oligonucleotide probes corresponding to the complementary sequences of the following mature miRNAs: *mir-221,* 5′-GAAACCCAGCAGACAATGTAGCT-3′; *let-7a-1,* 5′-AACTATACAACCTACTACCTCA-3′; and *miR-122a,* 5′-ACAAACACCATTGTCACACTCCA-3′. Probes were 5′-end labeled using the polynucleotide kinase in the presence of [γ-^{32}P]ATP. Hybridization was done at 37°C in 7% SDS/0.2 mol/L Na_2PO_4 (pH 7.0) for 16 h. Membranes were washed at 42°C, twice with 2× standard saline phosphate [0.18 mol/L NaCl/10 mmol/L phosphate (pH 7.4)], 1 mmol/L EDTA [saline-sodium phosphate-EDTA (SSPE)], and 0.1% SDS, and twice with 0.5× SSPE/0.1% SDS. Northern blots were rehybridized after stripping the oligonucleotides used as probes in boiling 0.1% SDS for 10 min. As a control for normalization of RNA expression levels, we hybridized blots with an oligonucleotide probe complementary to the *U6 RNA* (5′-GCAGGGGCCATGCTAATCTTCTCTGTATCG-3′). Digital images were acquired in the linear range of the scanner Fluor-S MultiImager (Bio-Rad). Intensities of band signals were quantified using the densitometric software Quantity One (Bio-Rad). miRNA amount was normalized with the corresponding *U6 RNA* in each sample.

Table 1. Characteristics of HCC patients enrolled in the study

Gender	Male	45
	Female	15
Etiology*	HCV	31
	HCV + BAb	6
	HBV + HCV	5
	HBV	5
	Ethanol	3
	HCV + ethanol	2
	HBV + ethanol	1
	BAb	1
	Cryptogenic	6
Focality †	Unifocal	42
	Multifocal	18
Size	≤3 cm	16
	>3 cm	44
Grading ‡	G_1	1
	G_2	20
	G_3	32
	G_4	7
α-Feto protein§	≤20 ng/dL	26
	20–400 ng/dL	19
	>400 ng/dL	15

Abbreviation: HBV, hepatitis B virus.
*BAb, antibodies against HBV; ethanol, history of ethanol abuse. Cryptogenic were those cases in which viral infections, ethanol abuse, hemochromatosis, Wilson's disease, α1-anti-tripsyn deficiency, primary biliary cirrhosis, autoimmune hepatitis, and primary sclerosing cholangitis were excluded.
† Unifocality or multifocality was assessed based on imaging techniques before surgery and by means of intraoperative ultrasound.
‡ Grading of the HCC was assessed according to Edmonson and Steiner's criteria (50).
§ α-Feto protein level was assessed before surgery.

Real-time RT-PCR analysis. The expression of mature miRNAs was assayed using the Taqman MicroRNA Assays (Applied Biosystems) specific for *hsa-mir-122a* (P/N: 4373151), *hsa-let-7a* (P/N: 4373169), and *hsa-mir-221* (P/N: 4373077) on 38 matched HCCs and cirrhosis. The expression level of *miR-122a* was measured also in HEP3B cells transfected with *miR-122a* (Ambion). Each sample was analyzed in triplicate. Reverse transcription reaction was done starting from 10 ng of total RNA and using the looped primers. Real-time PCR was done using the standard Taqman MicroRNA Assays protocol on the iCycler iQ Real-Time PCR Detection System (Bio-Rad). The 20 μL PCR included 1.33 μL reverse transcription product, 1× Taqman Universal PCR Master Mix, No AmpErase UNG (P/N 4324018; Applied Biosystems), 0.2 μmol/L Taqman probe, 1.5 μmol/L forward primer, and 0.7 μmol/L reverse primer. The reactions were incubated in a 96-well plate at 95°C for 10 min followed by 40 cycles of 95°C for 15 s and 60°C for 1 min. The level of miRNA expression was measured using *C*t (threshold cycle). The *C*t is the fractional cycle number at which the fluorescence of each sample passes the fixed threshold. The $\Delta\Delta C$t method for relative quantitation of gene expression was used to determine miRNA expression levels. The ΔCt was calculated by subtracting the *C*t of *U6* RNA from the *C*t of the miRNA of interest. The $\Delta\Delta C$t was calculated by subtracting the ΔCt of the reference sample (normal liver) from the ΔCt of each sample. Fold change was generated using the equation $2^{-\Delta\Delta C t}$. A pool of three normal livers was used for the standard curve calculation and as reference sample for the $\Delta\Delta C$t. The Taqman MicroRNA Assays for *U6* RNA (RNU6B, P/N: 4373381; Applied Biosystems) was used to normalize the relative abundance of miRNA.

miRNA target prediction. The analysis of miRNA predicted targets was determined using the algorithms TargetScan,[5] PicTar,[6] and miRanda.[7] To identify the genes commonly predicted by the three different algorithms, results of predicted targets were intersected using MatchMiner.[8]

Cell culture. SNU449 [American Type Culture Collection (ATCC) number CRL-2234] and HEP3B (ATCC number HB-8064) cell lines were cultured with Iscove's modified Dulbecco's medium with 10% fetal bovine serum and gentamicin.

Cell transfection with *miR-122a*. Stability-enhanced *miR-122a* precursor and negative control 1 ribo-oligonucleotides were from Ambion. The day before transfection, SNU449 and HEP3B cells were seeded in antibiotic-free medium. Transfection of miRNAs was carried out using Lipofectamine 2000 in accordance with the manufacturer's procedure (Invitrogen). The level of *miR-122a* expression in transfected HEP3B cell line was assayed by real-time RT-PCR (Taqman MicroRNA Assays) 24 h after transfection as described above.

Luciferase activity assay. The human *cyclin G1* 3′-UTR target site was amplified by PCR using the primers 5′-GCCTCAAACTGAATCCCATC-3′ (*CCNG1*-3UTR-F) and 5′-ATAAGCTTTTTGGCACAGTAAGGGCATC-3′ (*CCNG1*-3UTR-R) and cloned downstream of the luciferase gene in pMIR-REPORT luciferase vector (Ambion). This construct, named *pMIR-CCNG1,* was used for transfection in HEP3B cell line. HEP3B cells were cultured in 24-well plates and each transfected with 0.1 μg of either *pMIR-CCNG1* or pMIR-REPORT together with 0.01 μg of pRL-TK vector (Promega) containing *Renilla* luciferase and 30 pmol of *miR-122a* or negative control 1. Transfection

[5] http://genes.mit.edu/targetscan/
[6] http://pictar.bio.nyu.edu/
[7] http://cbio.mskcc.org/cgi-bin/mirnaviewer/mirnaviewer.pl
[8] http://discover.nci.nih.gov/matchminer/MatchMinerLookup.jsp

Table 2. miRNAs differentially expressed between human HCC and LC

miRNA	Symbol	Map	Normalized mean ratio HCC/LC*	Up-regulation or down-regulation in HCC	P †	SVM predictive strength ‡	Score for PAM prediction§	
							CE score	HCC score
let-7a-1	MIRNLET7A1	9q22.2	0.68	Down	0.0127	8.811		
let-7a-2	MIRNLET7A2	11q24.2	0.59	Down	0.0136	5.72		
let-7a-3	MIRNLET7A3	22q13.3	0.63	Down	0.0160	5.504	−0.0269	0.0331
let-7b	MIRNLET7B	22q13.3	0.74	Down	0.0149	6.434		
let-7c	MIRNLET7C	21q11.2	0.62	Down	0.0168	7.478	−0.0265	0.0326
let-7d	MIRNLET7D	9q22.2	0.70	Down	0.0307	6.434	−0.071	0.0874
let-7e	MIRNLET7E	19q13.4	0.77	Down	0.0245	3.811	−0.0139	0.0171
let-7f-2	MIRNLET7F2	Xp11.2	0.70	Down	0.0356	7.478	−0.0929	0.1143
let-7g	MIRNLET7G	3p21.3	0.71	Down	0.0307	4.332	−0.0575	0.0708
miR-122a	MIRN122A	18q21	0.63	Down	0.0135	6.434	0.2821	−0.3472
miR-124a-2	MIRN124A2	8q12.2	0.69	Down	0.0135	6.457	−0.0707	0.087
miR-130a	MIRN130A	11q12	0.50	Down	0.0339	8.938	0.1774	−0.2183
miR-132	MIRN132	17p13.3	0.75	Down	0.0152	6.065	−0.0478	0.0588
miR-136	MIRN136	14q32	0.58	Down	0.0191	8.135		
miR-141	MIRN141	12p13	0.74	Down	0.0389	6.318	−0.0468	0.0576
miR-142	MIRN142	17q23	0.51	Down	0.0082	9.228	−0.0182	0.0224
miR-143	MIRN143	5q32-33	0.72	Down	0.0127	8.938	−0.0533	0.0656
miR-145	MIRN145	5q32-33	0.53	Down	0.0126	8.938		
miR-146	MIRN146A	5q34	0.59	Down	0.0439	7.548	0.0333	−0.041
miR-150	MIRN150	19q13	0.47	Down	0.0101	10.34		
miR-155(BIC)	MIRN155	21q21	0.57	Down	0.0168	8.877		
miR-181a-1	MIRN213	1q31.2-q32.1	0.68	Down	0.0439	5.318	−0.0448	0.0551
miR-181a-2	MIRN181A	9q33.1-34.13	0.64	Down	0.0439	9.228	−0.0558	0.0686
miR-181c	MIRN181C	19p13.3	0.67	Down	0.0339	8.974	−0.0436	0.0537
miR-195	MIRN195	17p13	0.75	Down	0.0307	6.297	−0.0351	0.0431
miR-199a-1-5p	MIRN199A1	19p13.2	0.45	Down	0.0100	9.367		
miR-199a-2-5p	MIRN199A2	1q24.3	0.43	Down	0.0082	8.938		
miR-199b	MIRN199B	9q34	0.49	Down	0.0082	10.31		
miR-200b	MIRN200B	1p36.33	0.69	Down	0.0120	7.787	−0.0485	0.0597
miR-200b	MIRN200B	1p36.3	0.74	Down	0.0135	7.478	−0.0604	0.0744
miR-214	MIRN214	1q23.3	0.59	Down	0.0124	8.974		
miR-221	MIRN221	Xp11.3	1.49	Up	0.0339	4.396	−0.2452	0.3018
miR-223	MIRN223	Xq12-13.3	0.44	Down	0.0135	6.457	0.1443	−0.1776
pre-mir-594	MIRN594	7q34	0.55	Down	0.0500	5.318		

*HCC microarray data for each microRNA were normalized on respective cirrhosis; if not available, it was normalized on average of cirrhosis.
† P value derived from ANOVA in the GeneSpring software package.
‡ SVM prediction analysis tool (from GeneSpring 7.3 software package). Prediction strengths are calculated as negative natural log of the probability to predict the observed number of samples, in one of the two classes, by chance. The higher is the score, the best is the prediction strength.
§Centroid scores for the two classes of the PAM algorithm.

was done using LipofectAMINE 2000 and Opti-MEM I reduced serum medium (Life Technologies) in a final volume of 0.6 mL. Twenty-four hours after transfection, firefly and *Renilla* luciferase activity were measured using the Dual-Luciferase Reporter Assay (Promega). Each transfection was repeated twice in triplicate.

Western blot analysis. SNU449 and HEP3B cell lines were transfected in six-well plates with 100 pmol of *miR-122a* or negative control 1. After transfection, cells were cultured for 72 h and intermediate samples at 24 and 48 h were collected and analyzed by Western blot to assess cyclin G1 expression. A monoclonal antibody (clone 11C8, Novocastra Laboratories) against cyclin G1, diluted at 1:100, was incubated for 16 h at 4°C. A horseradish-conjugated secondary antibody (labeled polymer horseradish peroxidase antimouse, EnVision System, DakoCytomation) was incubated for 45 min at room temperature, and the corresponding band was revealed using the enhanced chemiluminescence method (Amersham). Digital images of autoradiographies were acquired with Fluor-S MultiImager, and band signals were acquired in the linear range of the scanner using a specific densitometric software (Quantity One). Images were calibrated against a reference autoradiography and given in relative density units. After autoradiography acquisition, the membranes were stripped and reprobed for 2 h at room temperature with anti-β-actin antibody (Santa Cruz Biotechnology, Inc.) to normalize protein loading. A ratio between cyclin G1 and β-actin corresponding bands was used to quantify cyclin G1 modulation by *miR-122a*.

Results

A miRNA expression signature differentiates HCCs from nonneoplastic liver tissue. We analyzed miRNA expression of 17 cases of HCC and 21 cirrhotic liver tissues using a miRNA microarray platform able to assess the expression level of 381

human miRNAs (19, 26). To identify the miRNAs that are differentially expressed between cirrhosis and HCC, we did a statistical comparison between the two groups of samples (combining a 1.3-fold change threshold and ANOVA $P < 0.05$). Thirty-five miRNAs emerged as differentially regulated in HCC tissue with respect to cirrhosis (Table 2). Based on these differentially expressed miRNAs, supervised hierarchical cluster analysis (by standard correlation) generated a tree showing a good separation between HCCs and LCs (Fig. 1). Two main groups on the opposite sides of the cluster emerged, one predominantly made of HCCs and the other of LCs. Some HCC and cirrhosis samples were included in the wrong group because they tended to cluster based on patient's individual profile instead of tissue type; for example, in the LC group, the HCC sample of patient 29 came together its matched cirrhosis, whereas LCs of patients 23 and 41 in the HCC group clustered together their matched HCCs. Two additional interposed smaller groups, mostly containing HCCs, showed an intermediate variation in the expression of miRNAs, and similarly to above, LCs clustered together their matched HCCs. The HCCs in the different groups did not show significant differences for etiology, focality, size, grading, and α-feto protein expression. To validate their ability to correctly distinguish HCC or cirrhosis tissue types, the 35 deregulated miRNAs were assayed using the algorithms SVM (25) and PAM (24). PAM correctly classified 86% of the samples and SVM classified 91% (Supplementary Table S3). These analyses proved that the miRNA "signature" was able to correctly predict most HCC and cirrhotic tissues and pointed out the more predictive miRNAs (Table 2).

Three of the deregulated miRNAs (*miR-221, let-7a-1,* and *miR-122a*) were further assayed by Northern blot and quantitative real-time RT-PCR for validation purposes (Supplementary Table S2). Northern blot analysis was done on a series of 40 HCC-LC patients, which confirmed the results obtained by microarrays. Cases analyzed by both microarrays and Northern blot displayed an identical expression pattern. Overall, Northern blot analysis revealed that *miR-221* was up-regulated in 83% of HCCs when compared with matched cirrhotic tissue, *let-7a-1* was down-regulated

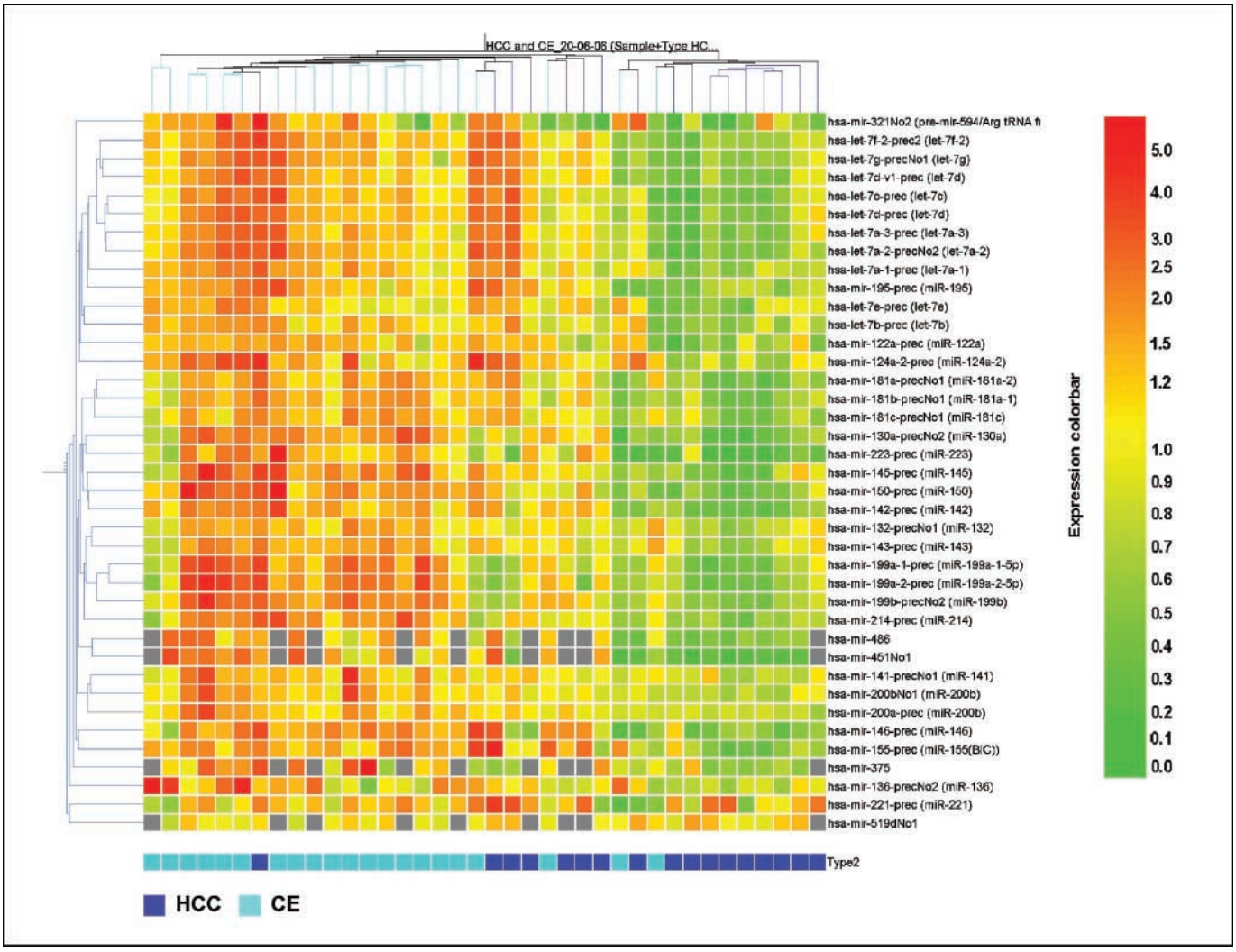

Figure 1. Classification of cirrhosis and HCC tissues according to a 35 miRNA expression signature. Cluster analysis of 21 cirrhosis and 17 HCCs (13 matched) based on the expression of the 35 miRNAs differentially expressed between cirrhosis and HCC that are listed in Table 2. *Rows,* miRNAs; *columns,* biological samples. For each miRNA, *red color* means an expression value higher than its average expression across all samples and *green color* means an expression value lower. In the lower bar, cirrhosis are represented by *cyan squares* and HCCs by *blue squares*.

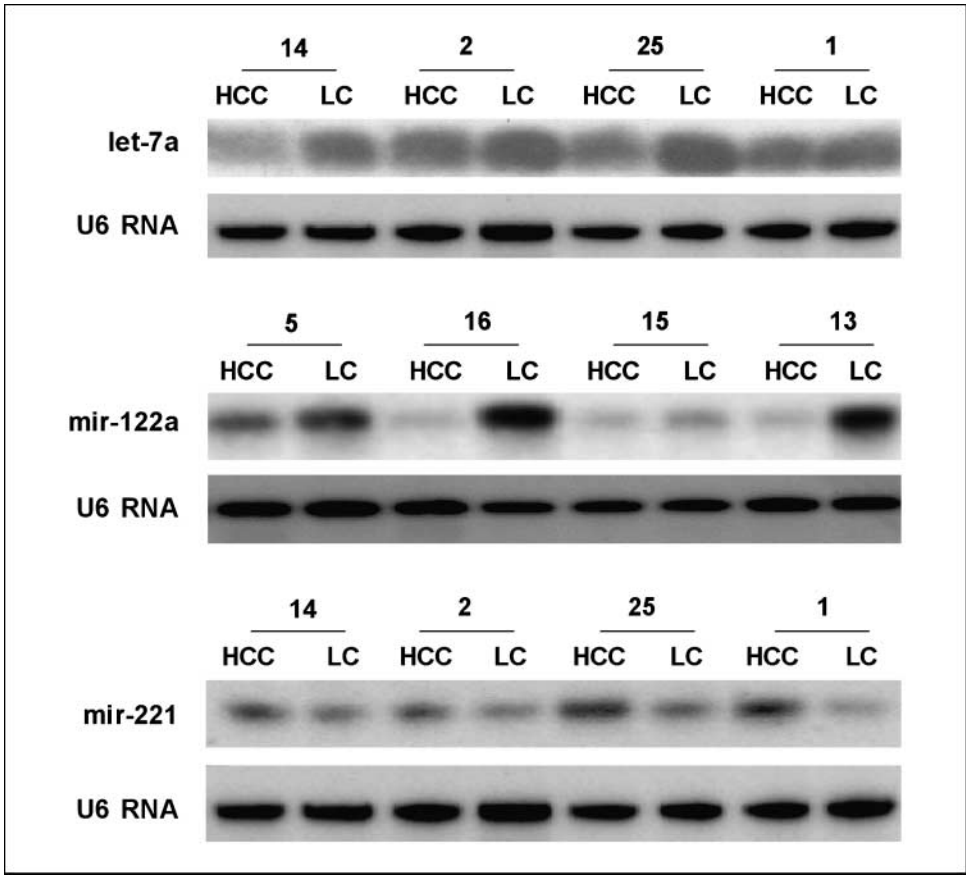

Figure 2. Representative results from Northern blots of *miRNAs let-7a, mir-221,* and *miR-122a*. Eight samples of matched HCC and LC. Northern blot analysis confirmed microarray results: *mir-221* is up-regulated, whereas *let-7a* and *miR-122a* are down-regulated in HCC versus matched cirrhotic tissue samples.

in 70% of HCCs, and *miR-122a* resulted down-regulated in 70% of HCCs. A selection of results is shown in Fig. 2. A miRNA quantification by RT-PCR was also done using the real-time Taqman assay for *miR-122a, let-7a,* and *miR-221* on 38 paired HCC-LC samples. Results confirmed the down-regulation of *miR-122a* and *let-7a* and the up-regulation of *miR-221* in tumors compared with cirrhosis (Supplementary Table S4).

***CCNG1* is a target of HCC-deregulated *miR-122a*.** Identification of miRNA-regulated gene targets is a necessary step to understand miRNA functions. *let-7* and *mir-221* were previously shown to be involved in cancer pathogenesis (27–31). Differently, the role of *miR-122a,* which represents the most abundantly expressed miRNA in human liver, in tumorigenesis remains unclear.

To begin unraveling the potential role of *miR-122a* in hepatocarcinogenesis, putative human protein-coding gene targets of *miR-122a* were identified by using miRanda, TargetScan, and PicTar algorithms. Results of the analysis are shown in Supplementary Table S5.

The gene for the *cyclin G1,* predicted by TargetScan and PicTar (Fig. 3*A*), was assayed as a target. After testing the HEP3B, SNU182, SNU398, and SNU449 cell lines for *miR-122a* expression by Northern blot and for cyclin G1 levels by Western blot, the human HCC cell lines SNU449 and HEP3B were chosen for assaying the *miR-122a* because *miR-122a* basal expression is undetectable in these cell lines and the 34-kDa cyclin G1 protein is easily detectable. Twenty-four hours after transfection, the level of *miR-122a,* detected by quantitative real-time RT-PCR, was similar to that of normal livers (fold change was 1.35 in transfected HEP3B versus 1.0 in normal liver; see Supplementary Table S4). Transfection of *miR-122a* in HEP3B and SNU449 caused a reduction in CCNG1 protein level of 55% and 25%, respectively. Cells transfected with the negative control did not exhibit any change in cyclin G1 levels (Fig. 3*B*).

To test whether the predicted *miR-122a* target site in the 3′-UTR of *cyclin G1* (*CCNG1*) mRNA was responsible for its regulation, we cloned the putative 3′-UTR target site downstream of a luciferase reporter gene (pMIR-*CCNG1*) and cotransfected this vector together with *miR-122a* or the scrambled Ambion negative control 1 into HEP3B cells. A *Renilla* luciferase vector (pRL-TK) was used as a reference control. Luciferase activity of cells transfected with *miR-122a* was decreased ~2-fold, a statistically significant difference, when compared with vector alone ($P = 0.0008$, t test) or with negative control (1.5-fold decrease; $P = 0.0038$, t test; Fig. 3*C*). Taken together, immunoassay and luciferase data provided strong indications that *CCNG1* is a target of *miR-122a*.

Furthermore, analysis of the expression of *miR-122a* and cyclin G1 in primary tumors confirmed the existence of an inverse correlation between the expression of *miR-122a* and cyclin G1 (Fig. 4). These data suggest that *miR-122a* may play a major role in the control of the level of cyclin G1 in liver tissues.

Discussion

In the recent years, several studies have shown that expression of miRNAs is deregulated in human malignancies (22, 28, 32). Identification of cancer-specific miRNAs and their targets is critical for understanding their role in tumorigenesis and may be important for defining novel therapeutic targets (18–22).

Here, we report an investigation on miRNA expression in human HCC. We discovered 35 miRNAs differentially regulated in HCC with respect to LC. The expression profile of this miRNA panel was able to discriminate the neoplastic versus the nonneoplastic liver tissue. Several miRNAs, differentially expressed in HCC, were previously found deregulated in other human cancers. Among these, the *let-7* family was shown to be down-regulated in various human cancers (22, 30, 31), *mir-221* was up-regulated in thyroid carcinomas and glioblastomas (29, 33), and *mir-145* was found down-regulated in colon and breast cancers (20, 34–36). Interestingly, *miR-122a,* a hepato-specific miRNA, resulted down-regulated in the majority of HCCs and in all examined HCC-derived cell lines. The high frequency of aberrant regulation of these miRNAs in HCC versus nontumor liver suggests that they might play an important role in hepatocarcinogenesis.

Other studies investigating the role of miRNA deregulation in human hepatocarcinogenesis have been reported. The microarray-based study by Murakami et al. (37) was done using a two-color approach, with a mixture of five human cell lines as reference. Possibly because of the different approach, none of the above-mentioned cancer-associated miRNAs emerged in their study and there was a limited overlap between our list of 35 and their list of 8 differentially expressed miRNAs: only *mir-195* and *mir-199a* were in common. In addition, because no accession to their raw data was available, it was not possible to compare their primary data with ours. Although based on a limited number of cases, but in agreement with our data, the article by Kutay et al. (38) revealed that *miR-122a* is significantly down-regulated in human and mouse HCC, confirming that down-regulation of *miR-122a* may play a role in hepatocarcinogenesis.

Understanding the tumor-promoting mechanism associated with miRNA deregulation remains a difficult task. In fact, although bioinformatic tools may help to reveal putative mRNA targets, experimental procedures are required for their validation. Only few studies have identified oncogenes whose level of expression is regulated by miRNAs: members of the *let-7* miRNA family can regulate all three members of the *RAS* oncogene family (30) and *mir-15a/mir-16-1* regulate *BCL2* (39). These findings support the idea that miRNA deregulation may be involved in cancer pathogenesis. Here, we show that *miR-122a* targets the *cyclin G1* mRNA, thus revealing a potential mechanism associated with liver tumorigenesis.

In fact, cyclin G1 deregulation is associated with genomic instability (40) and increased cyclin G1 levels have been described in colorectal cancer, breast cancer, and leiomyoma (41–43). Moreover, experimental evidences obtained in cancer cell lines and tumor xenografts have shown that suppression of cyclin G1 results in the inhibition of tumor growth through a reduction of

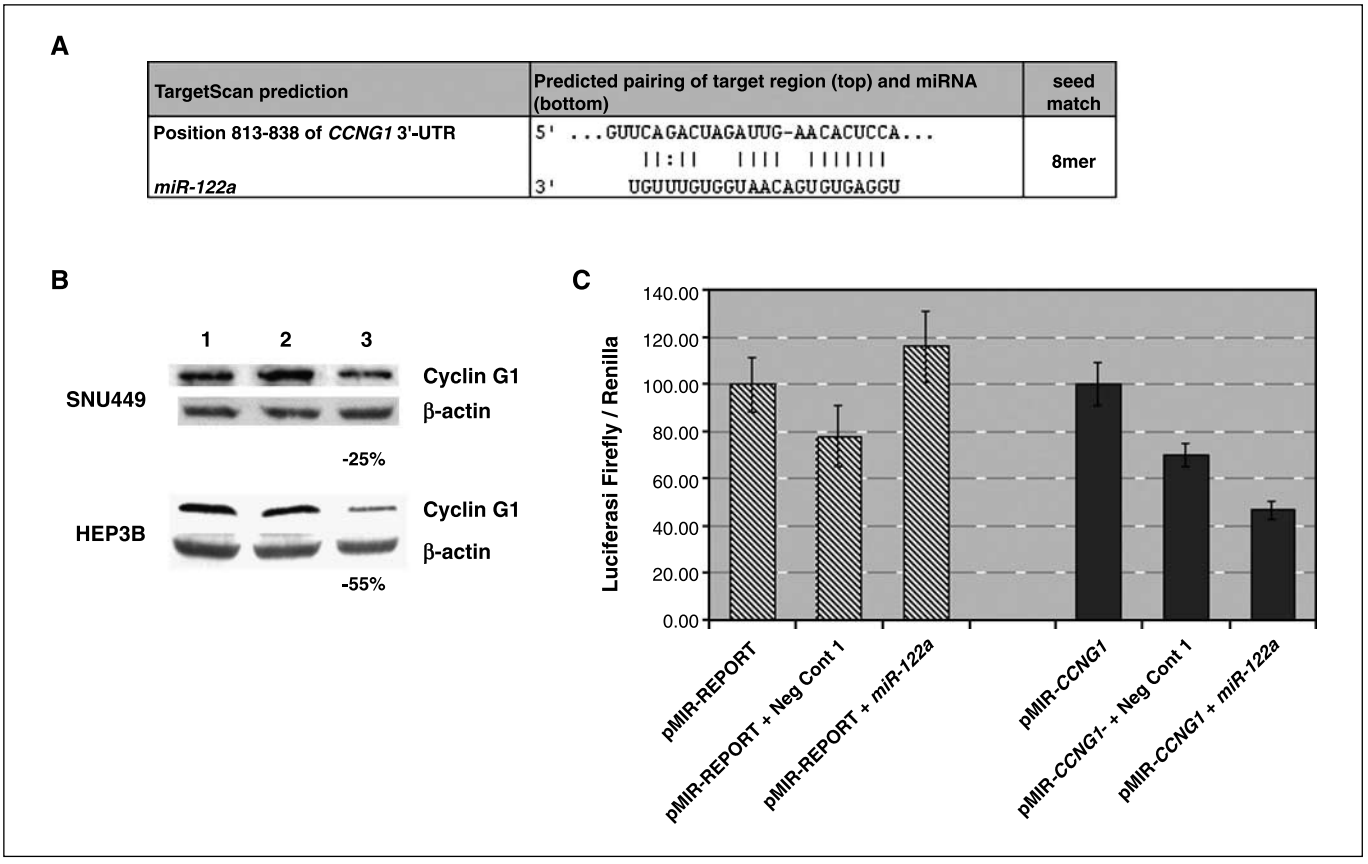

Figure 3. *Cyclin G1* is a *miR-122a* target. *A,* putative binding site of *miR-122a* in *cyclin G1* 3′-UTR region as detected by TargetScan. *B,* Western blot analysis of cyclin G1 expression after *miR-122a* transfection in HEP3B and SNU449 cell lines. Cells were collected 48 h after *miR-122a* transfection. *Lane 1,* cells treated with Lipofectamine 2000 alone; *lane 2,* cells treated with negative control 1; *lane 3,* cells treated with *miR-122a. C, cyclin G1* 3′-UTR regulates luciferase activity dependent on *miR-122a*. Expression of the firefly luciferase reporter activity is significantly reduced when pMIR-*CCNG1* vector, containing part of the 3′-UTR of the *cyclin G1* gene, is cotransfected together with *miR-122a* ($P = 0.0008$ versus vector alone, *t* test; $P = 0.0038$ versus negative control 1, *t* test). This reduction not only is not observed when control vector pMIR-REPORT is used but *miR-122a* causes an increase in luciferase activity of the pMIR-REPORT vector. Firefly luciferase activity was normalized on *Renilla* luciferase activity of the cotransfected pRL vector.

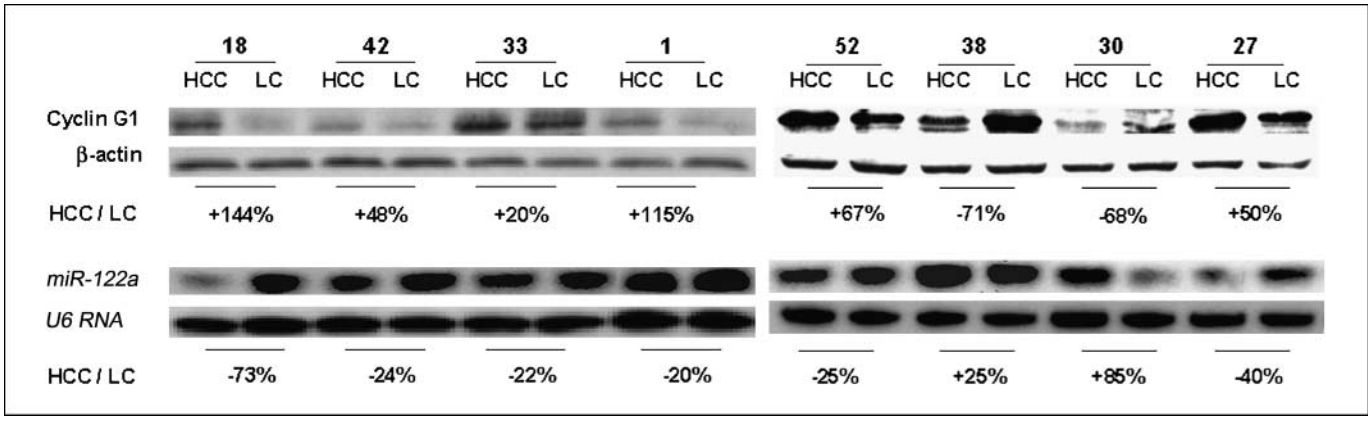

Figure 4. Inverse correlation between cyclin G1 and *miR-122a* expression in primary tumors. Tumors, selected for high or low *miR-122a* expression, were analyzed for cyclin G1 expression by Western blot. The level of expression of *miR-122a* and cyclin G1 was assessed as described in Materials and Methods. An inverse relationship was observed: when *miR-122a* is low, cyclin G1 is high; the opposite when *miR-122a* expression is high. The percentage of up-regulation or down-regulation was established first by normalizing cyclin G1 on β-actin expression and *miR-122a* on *U6 RNA* in each sample and then calculating the ratio between HCC versus matched LC.

proliferation and induction of apoptosis (44, 45). In experimental hepatocarcinogenesis, loss of cyclin G1 is associated with a significantly lower tumor incidence after carcinogenic challenge and cyclin G1–null hepatocytes enter S phase at a lower rate (46). Cyclin G1 is transcriptionally activated by p53 and p73, and, in turn, it negatively regulates p53 family proteins (47). Taken together, these data suggest that reduced levels of *miR-122a* in HCC may result in chromosomal instability through deregulation of cyclin G1 and, indirectly, p53-dependent pathways.

The importance of *miR-122a* for liver physiology is supported by the fact that *miR-122a* is specifically expressed in normal liver, accounting for 70% of the total liver miRNA population both in human and mouse. Hence, it is conceivable that its deregulation may have a significant effect on various liver functions (23). For example, *miR-122a* binds to the 5′ noncoding region of hepatitis C virus (HCV) RNA highly conserved in all the six HCV genotypes (23), suggesting that *miR-122a* is an essential element of the HCV replication-adaptation to the liver. It has been shown that functional inactivation of *miR-122a* leads to 80% reduction of HCV RNA replication, suggesting that loss of *miR-122a* in HCC may increase resistance of cancer cells to HCV replication. Furthermore, it has been reported that natural targets of *miR-122a* include several genes related with the adult liver phenotype and genes involved in cholesterol biosynthesis (48), suggesting that loss of *miR-122a* expression in HCC may be related to loss of hepatocyte differentiation.

This study helps to define cancer-associated miRNA-deregulated pathways involved in liver diseases, which could help to identify potential therapeutic targets. In addition, because liver can be effectively targeted by *in vivo* delivery of short RNAs, it represents a good model for the development of anticancer miRNA-based approaches of gene therapy as previously reported for other liver diseases (48, 49). Recognizing the miRNAs that are deregulated in human HCCs represents the first step for the development of experimental therapies of this type.

Acknowledgments

Received 12/14/2006; revised 3/21/2007; accepted 4/30/2007.

Grant support: Associazione Italiana per la Ricerca sul Cancro Regional grant, Ministero dell'Università e della Ricerca Scientifica and Comitato Sostenitori Project CAN2006 (M. Negrini), Associazione Italiana per la Ricerca sul Cancro Regional grant and Fondazione CARISBO (L. Bolondi), National Cancer Institute Program Project Grants (C.M. Croce), and Kimmel Foundation Scholar award (G.A. Calin). M. Ferracin is a recipient of a fellowship from Fondazione Italiana per la Ricerca sul Cancro.

The costs of publication of this article were defrayed in part by the payment of page charges. This article must therefore be hereby marked *advertisement* in accordance with 18 U.S.C. Section 1734 solely to indicate this fact.

References

1. Di Bisceglie AM. Issues in screening and surveillance for hepatocellular carcinoma. Gastroenterology 2004; 127:S104–7.
2. Llovet JM, Burroughs A, Bruix J. Hepatocellular carcinoma. Lancet 2003;362:1907–17.
3. Xu XR, Huang J, Xu ZG, et al. Insight into hepatocellular carcinogenesis at transcriptome level by comparing gene expression profiles of hepatocellular carcinoma with those of corresponding noncancerous liver. Proc Natl Acad Sci U S A 2001;98:15089–94.
4. Iizuka N, Oka M, Yamada-Okabe H, et al. Differential gene expression in distinct virologic types of hepatocellular carcinoma: association with liver cirrhosis. Oncogene 2003;22:3007–14.
5. Iizuka N, Oka M, Yamada-Okabe H, et al. Oligonucleotide microarray for prediction of early intrahepatic recurrence of hepatocellular carcinoma after curative resection. Lancet 2003;361:923–9.
6. Roberts LR, Gores GJ. Hepatocellular carcinoma: molecular pathways and new therapeutic targets. Semin Liver Dis 2005;25:212–25.
7. Lagos-Quintana M, Rauhut R, Lendeckel W, Tuschl T. Identification of novel genes coding for small expressed RNAs. Science 2001;294:853–8.
8. Lau NC, Lim LP, Weinstein EG, Bartel DP. An abundant class of tiny RNAs with probable regulatory roles in *Caenorhabditis elegans*. Science 2001;294:858–62.
9. Lee RC, Ambros V. An extensive class of small RNAs in *Caenorhabditis elegans*. Science 2001;294:862–4.
10. Miska EA. How microRNAs control cell division, differentiation and death. Curr Opin Genet Dev 2005;15: 563–8.
11. Ambros V. The functions of animal microRNAs. Nature 2004;431:350–5.
12. Farh KK, Grimson A, Jan C, et al. The widespread impact of mammalian MicroRNAs on mRNA repression and evolution. Science 2005;310:1817–21.
13. Houbaviy HB, Murray MF, Sharp PA. Embryonic stem cell-specific MicroRNAs. Dev Cell 2003;5:351–8.
14. Reinhart BJ, Slack FJ, Basson M, et al. The 21-nucleotide let-7 RNA regulates developmental timing in *Caenorhabditis elegans*. Nature 2000;403:901–6.
15. Griffiths-Jones S, Grocock RJ, van Dongen S, Bateman A, Enright AJ. miRBase: microRNA sequences, targets and gene nomenclature. Nucleic Acids Res 2006;34:D140–4.
16. Bentwich I, Avniel A, Karov Y, et al. Identification of hundreds of conserved and nonconserved human microRNAs. Nat Genet 2005;37:766–70.
17. Lewis BP, Burge CB, Bartel DP. Conserved seed pairing, often flanked by adenosines, indicates that thousands of human genes are microRNA targets. Cell 2005;120:15–20.
18. Calin GA, Liu CG, Sevignani C, et al. MicroRNA profiling reveals distinct signatures in B cell chronic lymphocytic leukemias. Proc Natl Acad Sci U S A 2004; 101:11755–60.

19. Liu CG, Calin GA, Meloon B, et al. An oligonucleotide microchip for genome-wide microRNA profiling in human and mouse tissues. Proc Natl Acad Sci U S A 2004;101:9740–4.
20. Iorio MV, Ferracin M, Liu CG, et al. MicroRNA gene expression deregulation in human breast cancer. Cancer Res 2005;65:7065–70.
21. Lu J, Getz G, Miska EA, et al. MicroRNA expression profiles classify human cancers. Nature 2005;435:834–8.
22. Volinia S, Calin GA, Liu CG, et al. A microRNA expression signature of human solid tumors defines cancer gene targets. Proc Natl Acad Sci U S A 2006;103: 2257–61.
23. Jopling CL, Yi M, Lancaster AM, Lemon SM, Sarnow P. Modulation of hepatitis C virus RNA abundance by a liver-specific MicroRNA. Science 2005;309:1577–81.
24. Tibshirani R, Hastie T, Narasimhan B, Chu G. Diagnosis of multiple cancer types by shrunken centroids of gene expression. Proc Natl Acad Sci U S A 2002;99:6567–72.
25. Furey TS, Cristianini N, Duffy N, Bednarski DW, Schummer M, Haussler D. Support vector machine classification and validation of cancer tissue samples using microarray expression data. Bioinformatics 2000;16:906–14.
26. Calin GA, Ferracin M, Cimmino A, et al. A MicroRNA signature associated with prognosis and progression in chronic lymphocytic leukemia. N Engl J Med 2005;353: 1793–801.
27. Ciafre SA, Galardi S, Mangiola A, et al. Extensive modulation of a set of microRNAs in primary glioblastoma. Biochem Biophys Res Commun 2005;334:1351–8.
28. He L, Thomson JM, Hemann MT, et al. A microRNA polycistron as a potential human oncogene. Nature 2005;435:828–33.
29. Pallante P, Visone R, Ferracin M, et al. MicroRNA deregulation in human thyroid papillary carcinomas. Endocr Relat Cancer 2006;13:497–508.
30. Johnson SM, Grosshans H, Shingara J, et al. RAS is regulated by the let-7 microRNA family. Cell 2005;120: 635–47.
31. Takamizawa J, Konishi H, Yanagisawa K, et al. Reduced expression of the let-7 microRNAs in human lung cancers in association with shortened postoperative survival. Cancer Res 2004;64:3753–6.
32. O'Donnell KA, Wentzel EA, Zeller KI, Dang CV, Mendell JT. c-Myc-regulated microRNAs modulate E2F1 expression. Nature 2005;435:839–43.
33. He H, Jazdzewski K, Li W, et al. The role of microRNA genes in papillary thyroid carcinoma. Proc Natl Acad Sci U S A 2005;102:19075–80.
34. Bandres E, Cubedo E, Agirre X, et al. Identification by real-time PCR of 13 mature microRNAs differentially expressed in colorectal cancer and non-tumoral tissues. Mol Cancer 2006;5:29.
35. Cummins JM, He Y, Leary RJ, et al. The colorectal microRNAome. Proc Natl Acad Sci U S A 2006;103: 3687–92.
36. Michael MZ, SM OC, van Holst Pellekaan NG, Young GP, James RJ. Reduced accumulation of specific microRNAs in colorectal neoplasia. Mol Cancer Res 2003;1: 882–91.
37. Murakami Y, Yasuda T, Saigo K, et al. Comprehensive analysis of microRNA expression patterns in hepatocellular carcinoma and non-tumorous tissues. Oncogene 2006;25:2537–45.
38. Kutay H, Bai S, Datta J, et al. Downregulation of miR-122 in the rodent and human hepatocellular carcinomas. J Cell Biochem 2006;99:671–8.
39. Cimmino A, Calin GA, Fabbri M, et al. miR-15 and miR-16 induce apoptosis by targeting BCL2. Proc Natl Acad Sci U S A 2005;102:13944–9.
40. Tanaka S, Diffley JF. Deregulated G1-cyclin expression induces genomic instability by preventing efficient pre-RC formation. Genes Dev 2002;16:2639–49.
41. Baek WK, Kim D, Jung N, et al. Increased expression of cyclin G1 in leiomyoma compared with normal myometrium. Am J Obstet Gynecol 2003;188:634–9.
42. Perez R, Wu N, Klipfel AA, Beart RW, Jr. A better cell cycle target for gene therapy of colorectal cancer: cyclin G. J Gastrointest Surg 2003;7:884–9.
43. Reimer CL, Borras AM, Kurdistani SK, et al. Altered regulation of cyclin G in human breast cancer and its specific localization at replication foci in response to DNA damage in $p53^{+/+}$ cells. J Biol Chem 1999;274: 11022–9.
44. Gordon EM, Liu PX, Chen ZH, et al. Inhibition of metastatic tumor growth in nude mice by portal vein infusions of matrix-targeted retroviral vectors bearing a cytocidal cyclin G1 construct. Cancer Res 2000;60: 3343–7.
45. Chen DS, Zhu NL, Hung G, et al. Retroviral vector-mediated transfer of an antisense cyclin G1 construct inhibits osteosarcoma tumor growth in nude mice. Hum Gene Ther 1997;8:1667–74.
46. Jensen MR, Factor VM, Fantozzi A, Helin K, Huh CG, Thorgeirsson SS. Reduced hepatic tumor incidence in cyclin G1-deficient mice. Hepatology 2003;37: 862–70.
47. Ohtsuka T, Ryu H, Minamishima YA, Ryo A, Lee SW. Modulation of p53 and p73 levels by cyclin G: implication of a negative feedback regulation. Oncogene 2003;22:1678–87.
48. Krutzfeldt J, Rajewsky N, Braich R, et al. Silencing of microRNAs *in vivo* with 'antagomirs'. Nature 2005;438: 685–9.
49. Song E, Lee SK, Wang J, et al. RNA interference targeting Fas protects mice from fulminant hepatitis. Nat Med 2003;9:347–51.
50. Edmonson HA, Steiner PE. Primary carcinoma of the liver: a study of 100 cases among 48,900 necropsies. Cancer 1954;7:462–503.